ChemSearch Journal 14(1): 54 – 65, June, 2023
Publication of Chemical Society of Nigeria, Kano Chapter

Received: 30/05/2023 Accepted: 29/06/2023
http://www.ajol.info/index.php/csj

Triazole Derivatives as Corrosion Inhibitors on Iron (110) Surface: A Theoretical Study

Nura Ishaq and *Magaji Ladan
Department of Pure and Industrial Chemistry, Bayero University, P.M.B. 3011, BUK, Kano, Nigeria
***Correspondence Email:** mladan.chm@buk.edu.ng

ABSTRACT

Corrosion inhibition potentials of triazole derivatives: 7-chloro-3-(2R,3S)-3-(2,4-difluorophenyl)-3-hydroxy-4-(1,2,4-triazol-1-yl) butane-2-yl] Quinozolin-1-one (TRC), 3-paranitro benzylidene amino-1,2,,4-triazole phosphate (TRP) and, 2-(2,4-difluorophenyl)-1-3-bis(1H-1,2,4-triazole-1-ol) (TRD) propan-2-ol have been studied theoretically by Quantum chemical calculations and molecular dynamics simulation. The values of Quantum chemical parameters E_{HOMO}, E_{LUMO}, energy gap (ΔE) , the energy of back donation (ΔE_{b-d}), dipole moment (μ), electronegativity (X), global hardness (η), ionization potential (I), electron affinity (A), number of electron transfer (ΔN), and interaction energy were determined. The Quantum chemical parameters calculated revealed that TRC molecule is relatively more nucleophilic in nature and potentially a better inhibitor. The Fukui indices values shows that the hetero atoms (N, O, and P) of the studied compounds are responsible for their inhibitive characteristics. Calculated binding energy and adsorption energies obtained from the Quenched molecular dynamics simulations, the relatively low values obtained were less 100 kcal/mol as such the molecules being weakly adsorbed onto iron (110) surface by Van der Waals forces of attraction and duly obeys physical adsorption mechanism in the order TRC >TRD > TRP. Bond length analyses were performed before and after adsorption, and the results demonstrated that the adsorption process on the Fe (1 1 0) surface had an impact on the bond length of specific bonds in the inhibitory molecules.

Keywords: Adsorption, Fukui indices, Molecular dynamics simulation, Quantum chemical parameters

INTRODUCTION

Corrosion is a global issue that hinders growth in both developed and developing nations (Meryem *et al.,* 2021). It has negative effects that aren't usually evident, like accidents, major financial losses, and a lack of productivity as a result of deteriorating infrastructure and industrial equipment (Al-otaibi *et al.*, 2022). Corrosion of significant industrial metal equipment, which has drawn a lot of attention in recent years, continues to be a source of concern for scientists, engineers, and researchers, as it impacts the metalworking, chemical, and oil sectors (Wei *et al*, 2008). Protection from corrosion prevents the waste of both resources and money during the industrial application and extends the life of the equipment (Khalid *et al.*, 2009).

The use of organic compounds as corrosion inhibitors is one of the most practical methods for the prevention of metallic corrosion in acidic media (Manjunath *et al.*, 2022). Heterocyclic organic compounds constitute a potential class of corrosion inhibitors; they contain heteroatoms such as oxygen, nitrogen, sulfur, and pi bonds in their molecules, through which they are adsorbed on the metal surface (Dheeraj *et al.,* 2020). Extracts of plants and other natural products have also been utilized for the protection of metals against corrosion (Lucky *et al.,* 2013). Researchers generally agreed that most of these plant extracts are green corrosion inhibitors because they are biodegradable, less toxic, and do not contain heavy metals (Kurapati and Yathism, 2018). The decrease in rate of corrosion indicates the adsorption of inhibitor molecules on metal or alloy surfaces is influenced by molecular size, geometrical shape, steric factor, and orientation of the electron donor site in the acid medium, thermal stability, and the electronegativity of heteroatoms present in the inhibitor molecule (Fater *et al.,* 2022). Therefore, the selection of an inhibitor is very important for the corrosion inhibition study (Ikpi *et al.*, 2017).

Fewer triazoles derivatives have been reported as corrosion inhibitors in different corrosive environments. Mhamed *et al.* (2013) published computational studies of the corrosion-inhibition efficiency of iron by three triazoles derivatives in acidic medium and the results show that, N-decyl-1, 2, 4-triazole, N-undecyl-1, 2, 4-triazole, and N-dodecyl-1, 2, 4-triazole have good inhibition efficiency, and the inhibition effect increases with the tail length of the saturated hydrocarbon. The calculated binding energy reached 276 kJ/mol for N-dodecyl-1, 2, 4-triazole. (Quraishi *et al.*, 2012) and colleagues reported 3-aryl substituted triazoles, namely, 4-amino-5-

phenyl-4H-1, 2, 4-triazole-3-thiol (ASTT), 4-amino-5-(2-hydroxy)-phenyl-4H-1, 2, 4-triazole-3-thiol (AHPTT), and 4-amino-5-styryl-4H-1, 2, 4-triazole-3-thiol (APTT), which were investigated for their inhibition action on corrosion of mild steel in 0.1 M HCl by electrochemical and weight loss methods, and the results showed that inhibition efficiency for all triazoles followed the order ASTT > AHPTT > APTT. The aryl styryl substituted triazole exhibited highest inhibition efficiency of95.2% at concentration of 5.72×10^{-4} mol L^{-1}.

In the present study, three triazole derivatives:7-chloro-3-(2R,3S)-3-(2,4-difluorophenyl)-3-hydroxy-4-(1,2,4-triazol-1-yl) butane-2-yl] Quinozolin-1-one (TRC), 3-paranitro benzylidene amino-1,2,4-triazole phosphate (TRP) and, 2-(2,4-difluorophenyl)-1-3-bis(1H-1,2,4-triazole-1-ol) (TRD) propan-2-ol were employed to examine their ability to prevent the corrosion of mild steel using quantum chemical calculations and molecular dynamics simulation. The choice of the compounds studied is therefore based, on their possible inhibitory power on the one hand, which can be linked to their structure containing several active adsorption centers, such as heteroatoms (N, O, P and S) and aromatic nuclei.

COMPUTATIONAL METHODS

Geometry Optimization of the Triazole Derivatives

The studied triazole derivatives (Fig.1) were drawn using ChemDraw Ultra 8.0 software. The compounds drawn were imported from ChemDraw into the BIOVIA Material Studio software, where the optimization process was carried out using DFT-D with restricted spin polarization on a DNP+ basis, and the local density functional was set to B3LYP in the gaseous phase (Yousefi *et al.,* 2023).

Quantum Chemical Parameter Calculation

Quantum chemical calculations of the investigated molecules were performed with the help of DFT and B3LYP (Becke's three parameters, Lee, Yang, and Par) (Banjo *et al.,* 2013).

Density functional theory is based on the principle that the energy of a molecule can be determined from its electron density instead of its wave function (Ladan *et al.,* 2012). In corrosion studies, DFT has also been found to be a powerful tool that can be used for the prediction of sites for electrophilic and nucleophilic attack (Eddy *et al.,* 2011). The programs were run in BIOVIA material studio software. The optimized geometry structure of the highest occupied molecular orbital (HOMO), the lowest unoccupied molecular orbital (LUMO), and electronic parameters like ionization potential (I), electron affinity (A), energy gap (ΔE), global electronegativity (X), global hardness (η), and global softness (σ), can be used to study the reactivity of the investigated molecules (Chahul *et al.,* 2019). According to Koopmann's theorem, the E_{HOMO} and E_{LUMO} energies were used to calculate the quantum indices using equations (Beeke, 1993).

$$I = -E_{HOMO} \quad (1)$$

$$A = -E_{LUMO} \quad (2)$$

$$\Delta E = E_{LUMO} - E_{HOMO} \quad (3)$$

$$\chi = \frac{(I + A)}{2} \quad (4)$$

$$\eta = \frac{(I - A)}{2} \quad (5)$$

$$\sigma = \frac{I}{\eta} \quad (6)$$

$$\Delta E_{b\text{-}d} = -\frac{\eta}{4} = \frac{1}{8}\ (E_{HOMO} - E_{LUMO}) \quad (7)$$

The calculated values χ and η of the inhibitor can be used to find the fractional number of the electron transferred (ΔN) from inhibitor molecules to the mild steel surface by equation (8):

$$\Delta N = \frac{\psi ms - \chi inh}{2(\eta ms + \eta inh)} \quad (8)$$

Where χ_{inh}, η_{MS}, and η_{inh} are the electronegativity and hardness values of mild steel and inhibitor molecules respectively. The theoretical values of the η_{ms} is 0 and the values of the work function (ψ) are 3.91, 4.82, and 3.88eV for (100), (110), and (111) planes of mild steel respectively (Pakiet *et al.,* 2019). Finally, the interaction energy ($\Delta\psi$) index of the inhibitor and mild steel can be calculated by equation (9).

$$\Delta\psi = \frac{(\chi ms - \chi inh)2}{2(\eta ms - \eta inh)} \quad (9)$$

Where theoretical values of χ_{ms} = 7eV and η_{ms} = 0Ev.

E_{HOMO} is associated with the ability of the inhibitor molecule to donate free electron pairs, and E_{LUMO} is related to the ability to accept electron from the mild steel (Shen and Koenig, 2019). Energy gap (ΔE) is another important DFT - based parameter to explain the interactions between the mild steel surface and the inhibitor molecules (Siaka *et al.,* 2014).The lower the value of (ΔE) the higher chemical reactivity and inhibition ability. Global hardness (η) and softness are important properties to measure the molecular reactivity and selectivity, low value of η and σ means higher adsorption (Sing and Quraishi, 2010). Number of electron transfer (ΔN), is reflective of inhibition efficiency, and if is negative means electron transfer take place from inhibitor to the mild steel surface (Shang, 1999).

Molecular dynamics simulation (MDS) analysis

Molecular dynamic simulation is an explanatory technique which is popular toward the studies of inhibitors and metal interaction (Swetha *et al.,* 2019). The interaction between triazole derivatives and iron (110) surface was investigated by molecular dynamic simulation using BIOVIA material studio software. In this study, Fe (110) surface have been chosen because it is well packed and most stable surface than other surfaces like Fe (111) and Fe (100) as reported in the literature (Taleeb *et al.,* 2011). The Forcite module optimized iron (110) single plane was expanded into different supercell depended on the size of the molecule and embedded in a deep vacuum slab. The optimized structures of the interaction of the inhibitor molecules with iron (110) surface were carried out using condensed-phase optimized molecular potentials for atomistic simulation studies (COM-PASS) force field, and smart algorithm in a simulation box measuring 1Å by 12 Å by 28 Å with a periodic boundary condition (Zulfareen *et al.,* 2016). The interaction energy ($E_{interaction}$) between iron (110) and triazole derivatives was calculated using equations 10 and 11,

$$E_{interaction} = E_{total} - (E_{surface} + E_{inhibitor}) \quad (10)$$

$$E_{binding} = - E_{interaction} \quad (11)$$

Where E_{total} is the total energy of iron (110) surface and adsorbed inhibitor molecules, $E_{surface+ inhibitor}$ refers to the overall energy of the metal surface and solution without inhibitor molecules and solution without inhibitor molecules and $E_{inhibitor}$ is the energy of the inhibitor molecules (Solmaz, 2014). The binding energy of the inhibitor molecule is the negative value of interaction energy (Ebenso *et al.,* 2010).

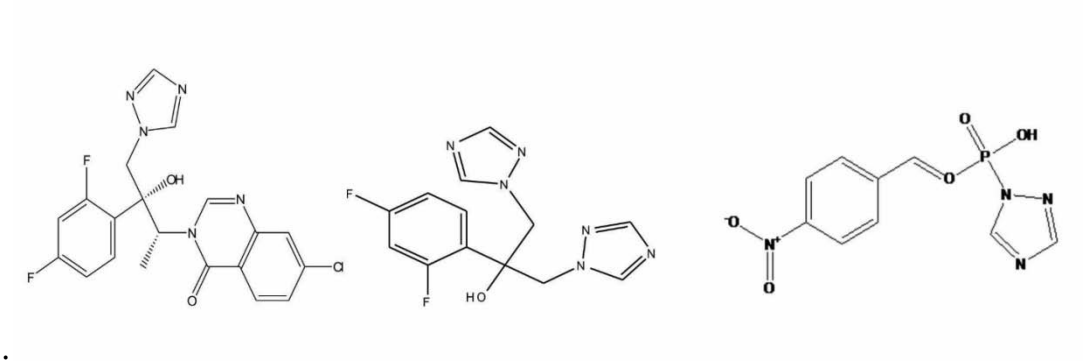

T R C T R D T R P

Figure 1: Molecular structures of the studied triazoles

RESULTS AND DISCUSSION

Quantum Chemical Calculations

To evaluate the relationship between triazole derivatives molecular structure and inhibitory performance, a quantum chemical computation was performed (Ahmad *et al.,* 2010). Fig.2 depicts the optimized molecular structures of each triazole, its highest occupied molecular orbital (HOMO), its lowest unoccupied molecular orbital (LUMO), and its electron densities. A closer look at the distributions shows that most of the HOMOs and LUMOs are located around the triazole ring. This would indicate that the preferred active sites for an electrophilic attack are located within the region around the nitrogen belonging to the benzotriazole ring.

HOMO and LUMO densities relate to portions of a molecule that might possibly contribute to electron-donating and electron-accepting abilities, respectively. The molecules total densities suggested that the entire molecule could improve corrosion inhibition on metal surfaces during the inhibition phase (Badr *et al.,* 2009). Based on increasing values of E_{HOMO}, studied inhibitors and molecules (Figure 2) are ranked TRC > TRP > TRD, while in the case of E_{LUMO} values, TRP > TRD > TRC. Another important quantum chemical parameter is ΔE (energy gap), defined as the difference between E_{LUMO} and E_{HOMO} (Al-Amiery *et al.,* 2022). The faster electrons transition from the HOMO level to the LUMO level in a molecule, the lower the energy gap of the molecule (Nnabuk *et al.,* 2011).

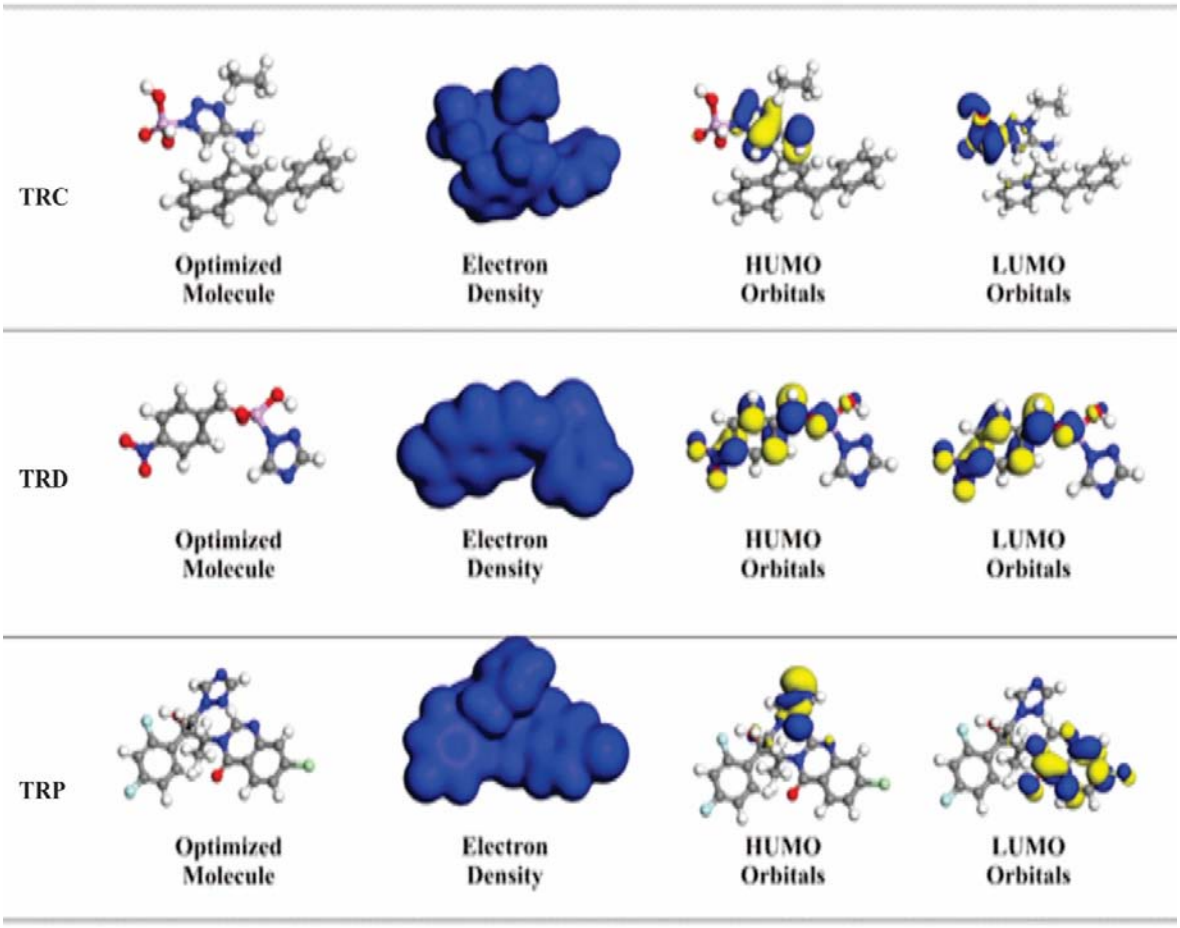

Figure 2: Total electron density and frontier orbitals of the studied triazoles derivatives

Key: The grey atom represents carbon, white represents hydrogen, yellow represents Sulphur, grey represents nitrogen, and light blue represents chlorine atom

Lower value of ΔE is associated with high chemical reactivity and inhibition ability. Based on the values of energy gap (ΔE), the order of molecules electron transfer potentials in this work is TRC > TRP > TRD.The molecule with highest ΔN content has the potential to be the most effective for inhibition corrosion. Amongst the compounds under study, TRP has the highest ΔN value (1.39).

Global hardness (η) and softness (σ) are related to selectivity and reactivity (Hegazy *et al.*, 2023). The adsorption of inhibitor molecule on mild steel surface is related with the value of (η) and (σ). Low value of (η) or high value of (σ) favor adsorption (Nhalalo *et al.*, 2023). Results presented from Table 1 with regard to hardness and softness, the trend in inhibition efficiency of triazole derivatives follows: TRC > TRD > TRP. Energy gap (ΔE), is also related to the hardness and softness of a molecule because soft molecule has low ΔE value while hard molecule has large ΔE, a soft molecule is expected to be more reactive than hard molecule due to smaller ΔE between the last occupied orbital and first virtual orbital (Siaka *et al.*, 2014). Hence, a potential corrosion inhibitor must have low value of (ΔE) and (η) but a high value of (σ) (Banallal *et al.*, 2023). From the triazole derivatives studied, TRC has the highest energy gap and therefore an indication of higher frequency of transfer of electrons between the molecules and the iron (1 1 0) surface, which are in order of TRC > TRD > TRP. Dipole moment (μ) is another important DFT-based parameter which can also provide information about the interactions between mild steel surface and inhibitors molecules (Amitha and Basu, 2011). The higher the dipole moment increase the inhibition efficiency due to large dipole-dipole interaction between inhibitor molecules and mild steel surface (Al-otabi *et al.*, 2014). The investigated molecules has larger value of dipole moment of 3.6, 4.1and 2.3 D for TRC, TRP and TRD respectively. Compare to water with dipole (1.8 D), hence studied molecules has higher dipole moment then water as such easily displace water molecule from mild steel surface (Ganapathi *et al.*, 2021). Energy of back donation (ΔE_{b-d}) is an important factor that explains the interaction of inhibitor molecules with the metal surface. When the global hardness value is positive and (ΔE_{b-d}) is negative, the interaction between the inhibitor molecules and iron (1 1 0) surface involves the transfer of charge from inhibitor molecules to the iron metal and vice versa (Fater *et al.*, 2022). Table 1 showed that global hardness values for both

investigated molecules are all positive. Based on the energy of back donation data, molecules inhibitory efficiency follows the trend TRC > TRP > TRD.

The interaction energy ($\Delta\psi$) is the contribution to the total energy that is caused by interaction between inhibitor molecule and iron metal surface (Manjunath *et al.*, 2022). The binding energies in Table 3, are all negative, showing that the combination processes of these corrosion inhibitors with iron (1 1 0) surface are exothermic and in order of TRP > TRC > TRD.

Table 1: Quantum Chemical Parameters of the molecules

Parameters	TRC	TRP	TRD
E_{HOMO} (e V)	-6.234	-5.564	-5.146
E_{LUMO} (e V)	-3.608	-5.071	-4.177
ΔE (e V)	2.284	0.493	0.969
μ (D)	3.6	4.1	2.3
I (e V)	6.234	5.564	5.146
X (e V)	4.921	5.318	0.4845
η (e V)	1.313	0.2465	0.969
σ (e V)$^{-1}$	3.748	2.25	3.310
ΔE_{b-d} (e V)	0.876	0.5643	0.123
ΔN (e V)	- 3.292	1.006	1.396
$\Delta\psi$ (e V)	-0.5643	-0.765	-0.365

Fukui Functions

The condensed Fukui function provides information about nucleophilic and electrophilic behavior of the corrosion inhibitor as well as charge distribution of the molecules (Aprael *et al.*, 2011). The nucleophilic and electrophilic Fukui function can be calculated using the finite difference approximation (FDA) as follows:

For electrophilic attack: $f_k^- = q_k(N) - q_k(N\text{-}1)$ (13)

For nucleophilic attack: $f_k^- = q_k(N+1) - q_k(N)$ (14)

For radical attack $f(k)^0 = \frac{q_k(N+1) - q_k(N-1)}{2}$ (15)

Where, $q_k(N)$, $q_k(N\text{-}1)$ and $q_k(N+1)$ are charge values of atom k for neutral, anion and cation state of the studied molecules respectively. The preferred site for the nucleophilic attack is the atom/ region in the molecule where the highest value of f^+ is found, while the site for electrophilic attack is the atom/ region in the molecule where the highest value of f^- is found (Bantiss *et al.*, 2002). Morell *et al*. (2011) have recently proposed a dual descriptor Δf (r) which is defined as the difference between the nucleophilic and electrophilic Fukui functions and is given by:

$$\Delta f(r) = [f_k^+ - f_k^-] \quad (16)$$

If $\Delta f(r) > 0$, then the site is favored for a nucleophilic attack, whereas if $I\Delta f(r) < 0$, then the site may be favored for an electrophilic attack. The calculated nucleophilic (f^+) and electrophilic (f^-) Fukui functions were reported in this work and the results of these with the highest values are shown in Table 2. The HOMO and LUMO orbitals are represented by nucleophilic and electrophilic Fukui functions, respectively as reported by Fater *et al.* (2022).

Table 2: Fukui Function Parameters of the Studied Molecules

		Nucleophilic attack (f^+)		Electrophilic attack (f^-)	
Compound	Atom	Mulliken	Hirshfeld	Mulliken	Hirshfeld
TRC	N_{16}	-0.059	0.054	0.321	0.114
TRD	N_{19}	-0.187	0.607	0.217	0.203
TRP	N_1	-0.076	0.022	-0.401	0.354

The Mulliken charge separation gives valuable information regarding the inhibition mechanism and mode of adsorption of the inhibitors on the metal or alloy surface (Thanh *et al.*, 2020). The atomic charges of the molecules were used to delineate the electronegativity process and transfer of charges from the investigated molecules, and the results are summarized in Table 2. If the Mulliken charges of the adsorbed center become more negative, the atom easily donates its electron to the vacant orbital of the metal surface (Banjo *et al.*, 2013).

Frontier orbital electron densities on atoms (Figure 3) provide a useful means for the detailed characterization of donor-acceptance interactions. In the case of a donor molecule, the HOMO density is critical to charge transfer (electrophilic density f_k^-), and in the case of an acceptor molecule, the LUMO density is important (nucleophilic electron density f_k^+) (Khalid *et al.*, 2009). In an analysis of the Fukui indices shown in Table 2, it is possible to observe that in each of the triazole derivatives, nitrogen atoms in the benzotriazole ring are the most susceptible sites for

electrophilic attacks. These sites present the highest values of f_k^-, while the pyridyl ring enhances the nucleophilic attack character of f_k^-.

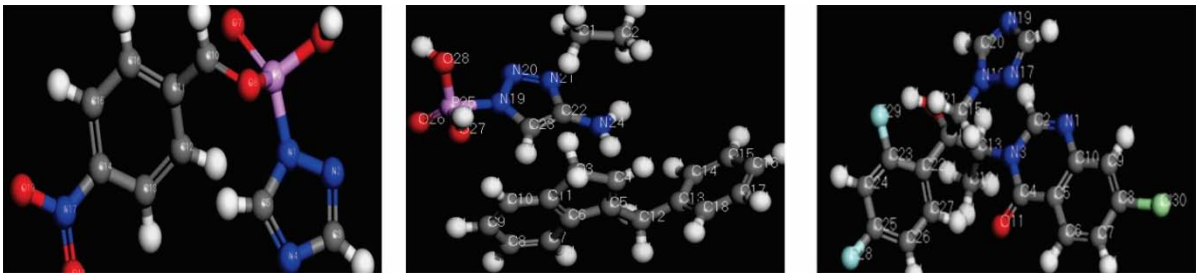

TRP **TRC** **TRD**

Figure 3: Labelled atoms of the studied compound

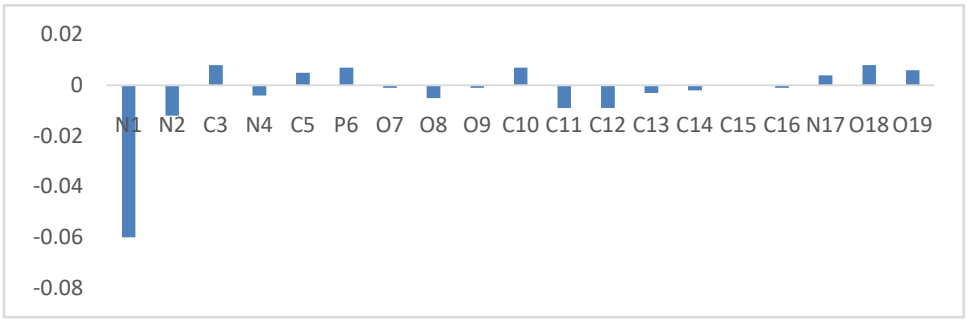

Figure 4a: Graphical representation of Fukui function for TRP

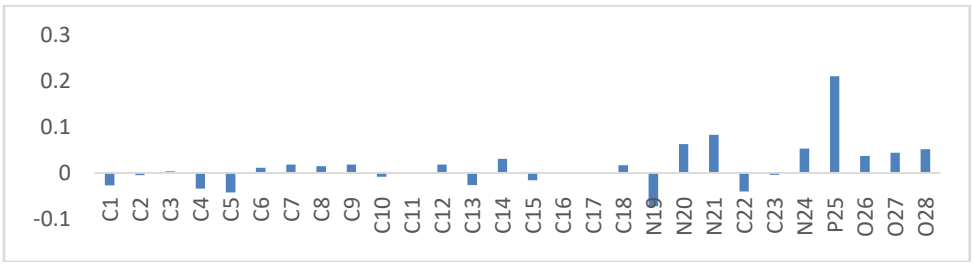

Figure 4b: Graphical representation of Fukui function for TRD

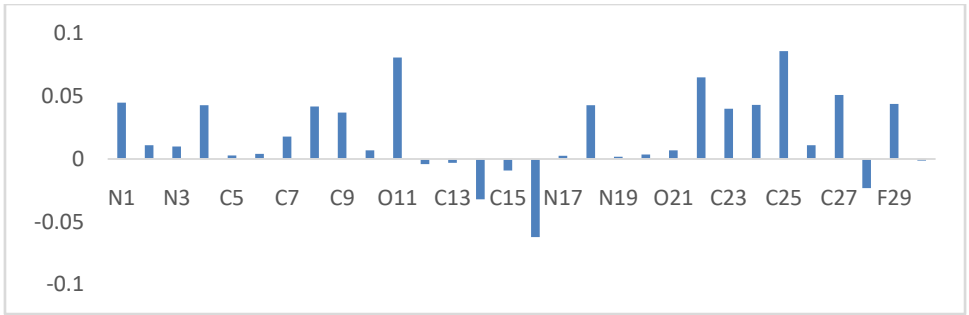

Figure 4c: Graphical representation of Fukui function for TRC

The Fukui function (f^2) is another important reactivity parameter. It's computed values are represented graphically in Figures 4a, b, and c and also in Table 3. From Figures 4a, b, and c and Table 3, we can say that in TRP 42.11% of the elements in Figure 4a exhibit positive values of second Fukui functions greater than zero ($f^2 > 0$), whereas 57.89 % of the elements exhibit negative values (f^2). According to these values for TRD, 67.86% of the elements in figure 4b showed positive values for second-order Fukui functions, while the remaining 32.14% showed negative values. Figure 4c and Table 3, the second-order Fukui function for TRC, have $f^2 > 0$ of 79.31 and f^2 of 20.69%. Conclusively, TRC is more nucleophilic than TRP, and TRD, as such, is more effective for inhibiting corrosion of iron metal surfaces (Fater *et al.*, 2022). In this case, the order of inhibitory effects is TRC > TRD > TRP.

Table 3: Percent second Fukui functions of the studied molecules

Molecule	f^{2+} %	f^{2-} %
TRC	79.31	20.69
TRD	67.86	32.14
TRP	42.11	57.89

Molecular Dynamic Simulation

Molecular dynamic simulation can provide more accurate information on the orientation and adsorption mode of the inhibitor (Fahimeh *et al.,* 2022). The adsorption ability is influenced by factors such as the presence of a functional group, steric factor, electronic structure, electron density at the donor site, and molecular size of the inhibitor (Quraishi *et al.*, 2012). Generally, any one or two of the above favorable factors define the orientation or binding mode of the inhibitor on the metal or alloy surface (Ibrahim *et al.*, 2022). As a consequence, the top and side views of the best adsorption configuration of the studied molecules on the Fe (110) surface are depicted in Figure 3. This figure reveals that the studied molecules adsorbed on the Fe (110) surface in planer or flat orientations, thereby covering the larger metallic surface area through their quinolone and hydroxyl nuclei.

Bond lengths and bond angles studies of the molecules could also be used as indicator (Zohren *et al.*, 2022). They can be assessed before and after molecules-metal interactions in order to establish the contact of each molecule with the metal surface (Wei-Hua *et al.*, 2008). The values reported in Tables 4a – c, were taken from the molecular structures corresponding to each molecules lowest energy after quenched simulation of the molecules on the iron (1 1 0) surface.

Table 4a: Variation in Bond length of the TRD Molecule before and after Simulation

Bond type	Length before adsorption (A^0)	Length after adsorption (A^0)
C_1-C_2	1.861	1.862
C_2-C_3	1.275	1.477
C_5-C_6	1.539	1.548
C_6-C_7	1.540	1.542
C_7-N_9	1.572	1.570
N_9-N_{10}	1.485	1.481
N_{10}-C_{11}	1.513	1.518
N_{12}-C_{13}	1.506	1.203
F_{25}-C_{22}	1.520	1.542
C_{21}-C_{22}	1.541	1.544

Table 4b: Variation in Bond length of the TRC Molecule before and after Simulation

Bond type	Length before adsorption (A^0)	Length after adsorption (A^0)
N_1-C_2	1.516	1.511
C_2-N_3	1.510	1.510
N_3-C_4	1.511	1.516
C_4-C_5	1.541	1.547
C_5-C_6	1.588	1.588
C_6-C_7	1.542	1.543
C_8-Cl_{30}	1.760	1.764
C_{23}-F_{29}	1.491	1.491

Table 4c: Variation in bond length of the TRP molecule before and after simulation

Bond type	Length before adsorption (A^0)	Length after adsorption (A^0)
N_1-C_2	1.484	1.481
N_2-C_3	1.513	1.513
C_3-N_4	1.509	1.509
N_4-C_5	1.506	1.507
C_5-N1	1.511	1.511
N_1-P_6	1.524	1.524
P_6-O_7	1.843	1.843
O_8-C_{12}	1.501	1.502
C_{12}-C_{13}	1.538	1.539
C_{13}-C_{14}	1.536	1.536
C_{14}-C_{15}	1.536	1.537
C_{14}-N_{17}	1.448	1.448
N_{17}-O_{19}	1.305	1.305

Table 5a shows the bond lengths of TRD before and after adsorption on the metal surface. From the results obtained, molecular interaction caused all the bond lengths in the molecule to be affected. When compared to variations in bond length for TRD and TRC, significant changes for TRP were not found. This might be due to the free side chain of TRD and TRC molecules, which makes it easier for them to bind with the metal surface and interact with the surface atom.

In Table 5b, TRC, five bond lengths: N_1-C_2, N_3-C_4, C_4-C_5, C_6-C_7, and C_8-Cl_{30} were all altered due to the adsorption process on the Fe (1 1 0) metal surface. In Table 5c, TRP, the bond lengths were not changed during adsorption of the molecule on the iron (1 1 0) surface except in N_1-C_2, N_4-C_5, O_8-C_{12}, C_{12}-C_{13}, and C_{14}-C_{15}

Table 5a: Variation in bond angle of the TRD molecule before and after simulation

Bond angle	before adsorption (^{0})	after adsorption (^{0})
N_1-N_2-C_5	126.151	126.010
N_2-C_3-N_4	110.668	110.511
N_{17}-O_{19}-O_{18}	129.973	129.861
C_{15}-C_{16}-C_{11}	119.478	116.994
C_{11}-C_{10}-O_8	128.980	128.532
O_{19}-N_{17}-O_{18}	129.973	129.654

Table 5b. Variation in bond angle of the TRC molecule before and after simulation

Bond angle	before adsorption (^{0})	after adsorption (^{0})
N_1-C_2-N_3	129.591	129.555
C_4-C_5-C_{10}	120.182	120.180
C_7-C_8-Cl_{30}	114.044	113.879
C_{23}-C_{22}-F_{29}	129.440	129.432
C_{10}-C_8-C_9	110.044	110.041
C_{25}-F_{28}-C_{26}	112.562	112.538
C_{14}-C_{22}-Cl_3	133.863	131.578

Table 5c: Variation in bond angle of the TRP molecule before and after simulation

Bond angle	before adsorption (^{0})	after adsorption (^{0})
N_{10}-N_9-C_{13}	129.408	129.403
C_{11}-N_{12}-N_{10}	134.697	134.688
C_6-C_7-C_{24}	119.170	117.657
C_{20}-C_{21}-F_{26}	133.408	133.306
F_{25}-C_{22}-C_{21}	113.488	113.098

Table 5a (TRD), b (TRC), and c (TRP) demonstrated the variation in bond angles before and after adsorption on an iron (1 1 0) surface, and the results showed that all the bond angles were altered as a result of adsorption. This is evidence of the interaction of the molecules atoms with the Fe (1 1 0) metal surface (Tsuru *et al.*, 2012). For all the molecules investigated (TRD, TRP, and TRC), the before and after simulation values of the molecules were not entirely planar, which suggested that the molecules might not have a flat orientation on the iron (1 1 0) surface to maximize surface adsorption. Since it is anticipated that the compounds will adopt a flat orientation on the iron (1 1 0) surface, all the inhibitor molecules bond angles are either $\pm 120^0$ (Fater *et al.*, 2022). This served as more evidence that, throughout inhibition processes, the inhibitor molecule exhibits sp^3 hybridization with primarily p-orbitals on the surface of the metal (Rocha *et al.*, 2010).

Results of the quenched dynamic simulation of each investigated molecule on the Fe (110) surface are shown in Table 5. It can be seen that the adsorption energies of TRC molecules is negative and greater than -100 kcal/mol$^{-1,}$ which means physical adsorption (Zulfaren *et al.*, 2016). The sequence of these compounds adsorption and binding energies is TRC > TRP > TRR, with TRC serving as the reference molecule and possibly being a better inhibitor than the others. This could be due to presence of pair of free electrons of the halogen (fluorine) can also interact with the metal surface other than the amine functional group found on the reference molecule. According to the Fater *et al.*(2022), pi – bonds and the relative size of the molecule also help in adsorption, which is why TRC and TRD adsorb more than TRP, Also, compounds containing more functional groups or heteroatoms (such as TRC and TRD) are more adsorptive than those with fewer functional groups (TRD).

The parameters obtained from molecular dynamic simulation are presented in Table 6. The adsorption energy was defined as the deformation energy for the adsorbate compound (Siaka *et al.*, 2014).

Table 6: Calculated parameters obtained from molecular dynamic simulation

Energy Parameters (kcal/mol)	TRC	TCR	TRD
Total kinetic energy	89.01	64.73	97.43
	±0.45	±2.71	±0.99
Total potential energy	98.34	-132.81	65.46
	±3.21	±0.44	±0.11
Energy of the surface	0.000	0.000	0.000
	±0.00	±0.00	±0.00
Energy of the molecule	102.12	-77.62	-157.9
	±0.00	±0.79	±0.02
Adsorption energy	-100.65	-69.64	- 98.99
	±0.00	±0.00	±0.00
Binding energy	00.65	69.64	98.99
	±0.00	±0.00	±0.00

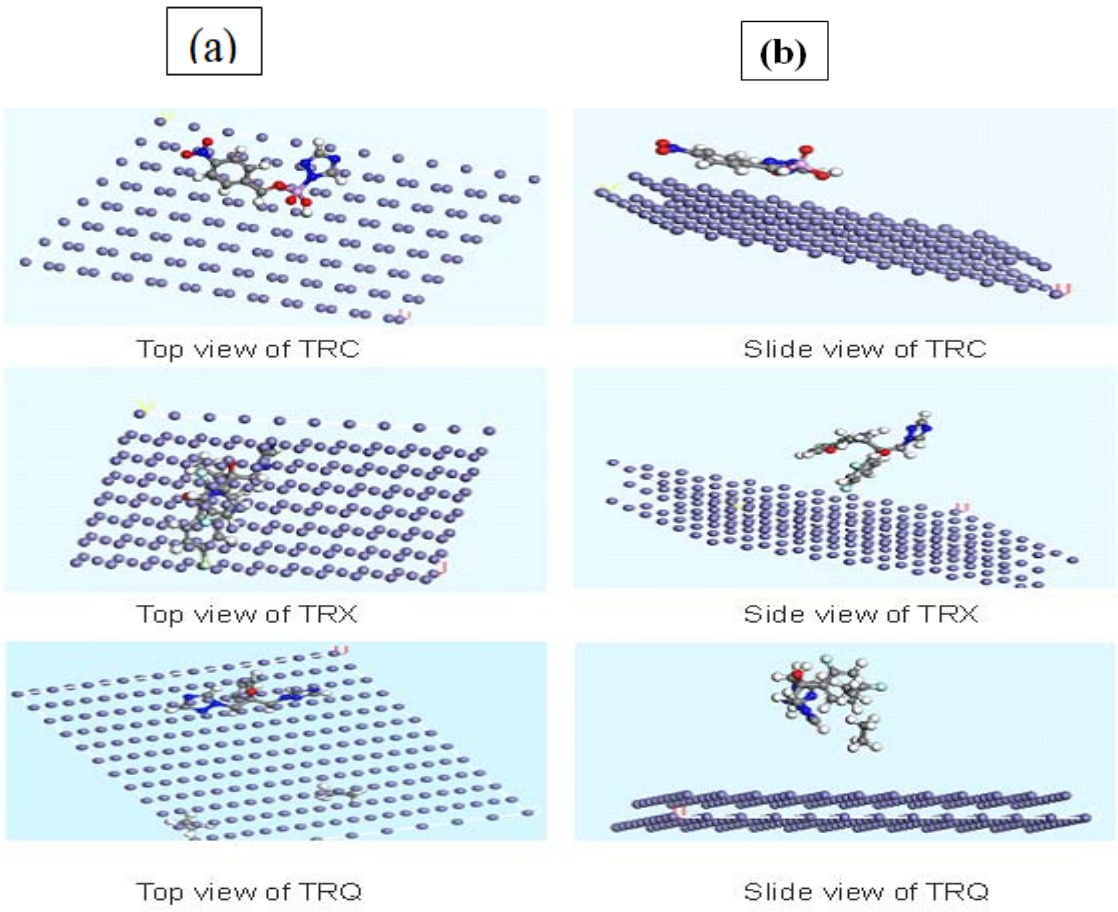

Figure 5: Molecular simulations for most favorable modes of adsorption obtained for the investigated inhibitor of TRP on Fe (110) surface side view (a) and top view (b)

CONCLUSION

The performance of various triazole derivatives on the Fe (110) surface as corrosion inhibitors has been investigated computationally using DFT and molecular dynamic simulation. Quantum chemical calculations for the compounds under study showed that TRC is predominantly more nucleophilic than the other 2. The hetero atoms in these molecules were discovered to be the likely point of contact with the Fe (110) surface after their local and global reactivity indices were examined by Fukui index analysis. Each molecule quenched in molecular dynamic simulation on the Fe (110) surface indicated the interaction was caused by van der Waals forces, which is a physical adsorption mechanism.

ACKNOWLEDGEMENT

The authors are very grateful to Dr Ayuba Abdullahi Muhammad, Department of Pure and Applied Chemistry, Bayero University, Kano state, Nigeria, for the BIOVIA Material Studio software installation.

REFERENCES

Ahamad I, Prasad R, Quraishi M (2010). Inhibition of mild steel corrosion in acid solution by Pheniramine Experimental and theoretical study. Corrosion Science, 52 (2). 3033-304

Al-Amiery A, Nadia B, Ahmad K, Walid K (2022): Experimental and quantum chemical investigation on the anticorrosion efficiency of a nicotine hydrazide derivative for mild steel in HCl. International journal of corrosion science 27(3).19: 6254.https//doi.org/10.3390/molecules27196254.

Al-otaibi M.S, Al- mayouf A.M, Khan A, Mousa A.A, Al-mazroa S. A, Alkhathlan H.Z (2014): Corrosion inhibitory Action of some plants extract on the corrosion of mild steel in acidic medium. Arabian journal of chemistry 7, 340-346.

Aprael, S. Y. Anees, A.K. Hadeel F.I (2011): Peach juice as an anti – corrosion inhibitor of mild steel. Journal of Anti-corrosion methods and materials 58(3), 116-119.https://doi.org/10.1108/00035591111 1.

Amitha R.B.E, Basu, J.B.B, (2011); Green inhibitors for corrosion protection of metals and alloys: An overview, international journal of corrosion science 201-243.

Arshadi M.R, Lashgari M, Parsafar G.A (2004). Cluster approach to corrosion inhibition Problems: interaction studies. Journal of Material chemistry and Physics 86, (2-3) 311-314. *https://doi.org/10.1016/j.matchemphys.2004.03.28*

Badr E, Gluradi K (2009). The role of some thiosemicarbazide derivatives as corrosion inhibitors for C- steel in acidic media. Corrosion Science, 51, 2529-2536.

Benallal A, Rbaa M, Rouifi Z, Galai M, Errahmany F (2023). Quinoxaline derivatives as newly acid corrosion inhibitors for mild steel: Synthesis, electrochemical, and theoretical Investigations. *Journal of Bio- and Tribo-Corrosion* 9, 109-126.

Bantiss F, Lagrence M, Traisnel M (2002); 2,5-bis(n-pyridyl)-1,3,4-oxadizoles as corrosion inhibitors for mild steel in acidic medium. *Corrosion Science* 56, 733-742.

Beeke, A. D. (1993). Density functional thermochemistry 111. The role of extract exchange. *Journal of chemical Physics*, 98, 5648-5652. https://doi/10.1063/1.464913

Bentiss F, Jama C, Mernani B, El- attari H, El-kadi L, Lebrini M, Traisnel M, Lagrenee M (2009). Corrosion control of mild steel using 3,5-bis (4-methoxyphenyl)-4-amino-1,2,4-triazole in normal hydrochloric acid medium. *Corrosion Science* 51(1), 1628-1635.

Breket G, Hur E, Ogretir C, (2002); Quantum chemical studies of some pyridine derivative as a corrosion inhibitor in acidic medium. *Journal of molecular science. Theochem*, 79,578.

Chahul H.F, Danat T.B, and Wuana R.A (2019). Corrosion inhibition studies on the influence of *colocasia esculenta* leaves extract on mild steel in 1.0 M HCl. *International journal of material and environmental science*. 10: 266-273.

Ebenso E, Isabirye D, Eddy N (2010). Adsorption and Quantum chemical studies on the inhibition potentials of some thiosemicarbazides for the corrosion of mild steel in acidic medium. *Int. J. Mol. Sci*, 11, 2473-2498. https://doi.org/10.3390/ijms11062473

Eddy N.O, Siaka A, Femi E.A, Magaji L (2011). Chemical Information From GC-MS Studies of Ethanol Extract of *Andrographis paniculata* and their Corrosion Inhibition Potentials on Mild Steel in HCl Solution. *International Journal of Electrochemical Science*, 6(4316-4328)

Eddy N.O, Femi E.A, Casmir E, Gimba K, Nkechi O, Ibisi E, Ebenso E (2011). QSAR, Experimental and computational chemistry simulation studies on the inhibition potentials of some amino acids for the corrosion of mild steel in 0.5 M HCl. *International Journal of Electrochemical Science*, 6(931-957).

Fahimeh A, Erfan R, Mohammad D, Seeram R (2022). Recent advances on the corrosion inhibition behavior of Schiff base compounds on mild steel in acidic media. *Chemistry Select*, 1(31)Wiley –Vch-gmbh

Fater I, Abdulfatah S.M, Abdullahi A.M (2022). Quinazoline derivatives as corrosion inhibitors on aluminum metal surface. A theoretical study. *Advanced Journal of Chemistry Section* A, 2023, 6(1), 71-84

Ganapathi R.S, Vengatesh G, Thamaraiselvi M, Prabakaran R, Thailan V, Muthuvel I, (2021). Experimental and computational approach of an expired antibiotic drug kynurenic acid as an efficient corrosion inhibitor for mild steel in HNO_3 medium. *Journal of Iranian Chemical Society*, 5(42-54)

Guo L, Hundong W, Wei S, Faheem A, Yuanhua L, Riaradh M (2023): Experimental and theoretical studies of the corrosion inhibition performance of a Quaternary phosphonium- Based ionic liquid for mild steel in HCl medium. *Sustainability*, 15, 3103. *https//doi.org/10.3390/sui5043109*

Hegazy M, Haiba N, Award K, Maghoub F (2023). Synthesis, DFT, molecular dynamics, and monte carlo simulation of a novel thiourea derivatives with extraordinary inhibitive properties for mild steel in 0.5 M H_2SO_4 solution. *Physical Chemistry Chemical Physics*: Pccp 5(65-73)

Ibrahim B, Jmiami A, Bazzi L, Issami S (2020). Amino acid and their derivatives as Corrosion inhibitors for metal and alloys. *Arabian Journal of Chemistry* 13, 740-771

Ikpi M.E, Abeng F.E, Okonkwo B.O (2017): Experimental and computational study of levofloxacin as corrosion inhibitor for carbon steel in acidic media. *World News of Natural Sciences*, 9(79-90).

Khalid K.F, Sahar A.A, Fadl-Allah, Hammouti. B (2009): Some benzotriazole derivatives as corrosion inhibitors for copper in acidic medium; Experimental and Quantum chemical molecular dynamics approach. *Material Chemistry and Physics* 11(7):148-155.

Kurapati Yathism M.S (2018): Molecular dynamics simulation to understand behavior of corrosion inhibitors in bulk aqueous phase and near metal-water interface. *Dissertation submitted to Department of Engineering and Technology Russ College*.

Lucky C, Isiah, Nkem I (2023): Evaluation of mild steel corrosion protection in 1 M HCl solution by vildagliptin: Experimental and theoretical studies. *International scientific SSS Journal*. WSN 177(2023) 51-67

Magaji L, Ameh P.O, Eddy N.O, Uzairu A, Siaka A.A, Habib S, Ayuba A.M, Gumel S.M (2012): Ciprofloxacin as corrosion inhibitors for mild steel – Effects of concentration and temperature. *International Journal of Modern Chemistry*: 2(2): 64-73

Manjunath H, Nayak S.P, Narasimha R (2022): Microwave-assisted extraction of *swietenia macrophylla* fruit shell and its application in corrosion inhibition for mild steel in 0.5 M HCl pickling environment. *Indian Academy of Sciences .https.//doi.org/10.1007/s 12046-002-02066-z*

Meryem H, Lahoucine B, and Salah-Eddine S (2021): An Overview on the performance of 1, 2, 3-triazole derivatives as corrosion inhibitors for metal surfaces. *International Journal of Molecular Sciences*. 23,(1), 16.https://doi.org/10.3390/ijms23010016.

Mhamed T, Najat H, Dage S, Hassan R (2013): Computational studies of the corrosion inhibition efficiency of iron by triazole surfactants. *International Journal of Quantum Chemistry*, 113, 1365-1371. Dol:10.1002/qua.24310

Nnabuk H, Eddy O, Benedict I, Ita A (2011). QSAR, DFT and quantum chemical studies on the inhibition potentials of some carbozones for the corrosion of mild steel in HCl. *J.Mol*.17,359-376. https://doi 10.1007/s00894-010-0731-7

Nhalalo M, Dube J, Unarine T, Simon S, Mnyakeni M, Lutendo C (2023). Investigation of synthesized ethyl-(2-(5-arylidine-2,4-dioxothiazolidin-3-yl) acetyl) butanoate as effective corrosion inhibitor for mild steel in 1 M HCl: A gravimetric, electrochemical, and spectroscopic study. International journal biological macromolecules PMID: 2598143 *Reviews*. hppts://doi.org/10.1016/j.heliyon.2023.el14753

Pakiet M, Tedim J, Kowalczyk I, Brycki B (2019) ; Effectiveness of O-bridged cationic Gemini surfactants as corrosion inhibitors for stainless steel in 3 M hydrochloric acid: Experimental and theoretical studies. Journal of molecular liquid 249. 1113-1124.

Quraishi M.A, Sudheer K.R, Ansari, Ebenso E (2012). 3-Aryl substituted triazole derivatives as new and effective corrosion corrosion inhibitors for mild steel in hydrochloric acid solution. International Journal of electrochemical Science 7(2012) 7476-7492

Rocha F.G, Nnanna L, A, Owate I.O, Oguizie W. (2010); Inhibitive and adsorptive properties effects of *parinari polyandra* on mild steel corrosion in aqueous sulfuric acid. *Journal of Pure and Industrial Chemistry* 9(6), 125-134.

Shang Y.C (1999); A study of the effect of some inhibitors on the corrosion rate of austenitic stainless steel in sulfuric acid. Journal of chemical engineering science42: 337-351

Shen C, Alvarez V, Koenig J.D.B (2019). Gum Arabic as corrosion inhibitor in the oil industry; experimental and theoretical studies: *Journal of corrosion engineering science and technology* 54(5), 444-454

Siaka A.A, Eddy N.O, Idris S.O. Magaji L (2014); Ampicillin potentials as corrosion inhibitor:Fukui function calculations using B_3-LYP exchange correlation. *Nigerian Journal of Chemical Research*. 19 (4): 12-25.

Singh A, Singh V.K, Quraishi M.A (2010); Effects of fruit extract of some environmental benign green corrosion inhibitors on corrosion of mild steel in Hydrochloric acid solution. *Journal of Material and Environmental Sciences* 4 (3), 162-174.

Solmaz R. Investigation of corrosion inhibition mechanism and stability of vitamin B1 on mild steel in 0.5 M HCl solution. *Corrs. Sci*. 2014, 81, 75-84.https://doi.org/10.1016/j.corsci.2023.12.006

Swetha G. A, Sachin H.P, Guruprasad M.A, Prasanna J, (2019); Study of corrosion inhibition of mild steel by capacitabine in hydrochloric acid media. *International Journal of Industrial Chemistry* 10, 17-30.

Taleb H.I, and Mohamed Zour A, (2011); Corrosion inhibition of mild steel using fig leaves extract in hydrochloric acid solution. *International Journal of Electrochemical Science* 6(12), 6442-6455.hppts://doi.org/10.1016/S11452-3981,19692-1

Takriff M, Gadafi S, Mohd H, Wan R, Makarim H, Lina M, (2021). Insight into corrosion behavior of a 5-mercapto-1,2,4-triazole derivative for mild steel in hydrochloric acid solution: Experimental and DFT Studies. *Lubricants* 9, 122. https://doi.org/10.3390/lubricants9120122

Thanh L, Nguyen S.H, Phan M, Quoc B, Dao Vinh A (2020): Combined experimental and Computational studies on corrosion inhibition of *Houttuynia cordata* leaf extract for steel in HCl medium. *Journal of molecular liquids*. So167-7322(20) 32460-0 *https//doi.org/10.1016/j.molliq.2020.113787*

Tsuru F.G, Mu G.L, Liu X, (2005); A study of inhibition of iron corrosion in HCl solutions by some amino acids. *Journal of corrosion science 47,* 1932-1952.

Wei- Hua LI, Qiao He, Sheng-Tao, Sheng- tao Zhang and Chang- Ling Pei (2008): Some new of triazole derivatives as inhibitors for mild steel corrosion in acidic medium. International *Journal of Applied Electrochemistry* 38,289-295

Yousefi Y, Oucheikh L, Ou-ani O, Jabba M, Oubair A, Znini M, Hammouti B. (2023). Synthesis, Characterization and Corrosion Inhibition Potential of Olefin Derivatives for Carbon Steel in HCl: Electrochemical and DFT investigations, *Mor. J. Chem*, 14(1), 155-187.*Doi:https//doi.org/10.48317//IMIST.PRSM/morjchem-v11i1.37306*

Yurt A, Breket G, Ogretir C (2005). Quantum chemical studies on inhibition effect of amino acids and hydroxyl carboxylic acids on pitting corrosion of aluminum alloy 7075 in HCl solution. *Journal of Molocular Structure*, 725-215-221.

Zohreh M, Mahdieh K, Parsa H, Hamid R.S, Asghar A , Hamid S (2022). Novel 1,2,3-triazole-based benzothiazole derivatives: Efficient synthesis, DFT, molecular docking, and ADMET studies. *Molecules* 2022,27,8555. https://doi.org/10.3390/molecules2723855

Zulfareen N, Kannan K, Venugofal T, Gnanvel S (2016);Synthesis, characterization and corrosion inhibition efficiency of N-(4-(Morpholinomethylcarbamoyl phenyl furan-2-carboxamide for brass in HCl medium. *Arabian Journal of Chemistry* 15(654-650).